

## Bulk Electronic State of SrTiO<sub>3-δ</sub> Probed by Resonant Soft-X-Ray Emission Spectroscopy

Tohru HIGUCHI, Yoshiro YOKOYAMA, Shu YAMAGUCHI<sup>1</sup>, Akiko FUKUSHIMA<sup>2</sup>, Shik SHIN<sup>2,3</sup> and Takeyo TSUKAMOTO

Department of Applied Physics, Tokyo University of Science, Tokyo 162-8601, Japan

<sup>1</sup>Department of Materials Science, University of Tokyo, Tokyo 113-8656, Japan

<sup>2</sup>Institute for Solid State Physics, University of Tokyo, Chiba 277-8581, Japan

<sup>3</sup>RIKEN, Hyogo 679-5143, Japan

(Received March 13, 2003; accepted for publication April 14, 2003)

The bulk electronic state of SrTiO<sub>3-δ</sub> has been studied by means of soft-X-ray emission spectroscopy (SXES) and photoemission spectroscopy (PES) in the Ti 2*p* energy region. The PES spectrum shows two peaks in the energy region immediately below the Fermi level ( $E_F$ ), which sites in an energy band gap. Both peaks correspond to a coherent part at  $E_F$  and to an incoherent part at a binding energy of approximately 1.5 eV. In  $t_{2g}$ -resonanced SXES spectra, Raman scattering of the  $\delta t_{2g}$  peak occurring near 2.0 eV arises from a  $d$ - $d$  transition from the occupied incoherent band to the unoccupied coherent band. The Raman shift reflects the half of the intra-atomic Coulomb energy ( $U_{dd}/2$ ). [DOI: 10.1143/JJAP.42.L592]

KEYWORDS: SrTiO<sub>3-δ</sub>, soft-X-ray emission spectroscopy (SXES), electronic structure,  $d$ - $d$  transition, photoemission spectroscopy (PES), incoherent, coherent

SrTiO<sub>3</sub> is a typical perovskite-type oxide with a band gap of 3.2 eV. The SrTiO<sub>3</sub> crystal has  $n$ -type conductivity due to doping with electric carriers and becomes a superconductor. Such electron doping is known to transform insulating SrTiO<sub>3</sub> readily into a metallic state even with a very small extent of doping.<sup>1–4</sup> Doping can be achieved by altering any of the three sublattices, namely, those of Sr<sup>2+</sup>, Ti<sup>4+</sup> and O<sup>2-</sup>. In particular, La<sup>3+</sup> substitution at the Sr<sup>2+</sup> site (Sr<sub>1-x</sub>La<sub>x</sub>TiO<sub>3</sub>) and Nb<sup>5+</sup> substitution at the Ti<sup>4+</sup> site (SrTi<sub>1-x</sub>Nb<sub>x</sub>O<sub>3</sub>) have been extensively studied.<sup>1–4</sup> These samples are used as a substrate for the thin film deposition of ferroelectrics and superconductors because of their similar crystal structures and good lattice matching. On the other hand, SrTiO<sub>3-δ</sub> might also be expected to be used for substrate for the thin film deposition.

Recently, the electronic structure of the doped SrTiO<sub>3</sub> has been extensively studied by means of photoemission spectroscopy (PES).<sup>5–11</sup> In a lightly doped region, there will be no electron correlation among the doped electrons since the probability of electron-electron scattering is negligibly small. The PES spectra of SrTi<sub>1-x</sub>Nb<sub>x</sub>O<sub>3</sub> and Sr<sub>1-x</sub>La<sub>x</sub>TiO<sub>3</sub> show two peaks in the band gap energy region, which are generally believed to be respectively a coherent band at Fermi level ( $E_F$ ) and an incoherent band at a binding energy of ~1.5 eV that is attributed to a remnant of the lower Hubbard band. The band calculation based on a rigid-band filling model cannot reproduce the peak at ~1.5 eV,<sup>5,6</sup> though the O 2*p* valence band shows a good agreement with the PES spectra. The coherent band corresponds to the impurity band, which is expected from the rigid-band model. However, the origin of the incoherent band has not been clarified thus far. In recent years, it has been proposed that the incoherent band at ~1.5 eV is caused by a polaronic feature<sup>5,6</sup> or a surface structure that is created due to the degree of correlation and disorder in the surface.<sup>11–14</sup> A similar structure has also been observed in the PES spectrum of SrTiO<sub>3-δ</sub>.<sup>10,11</sup>

In this letter, we present soft-X-ray emission (SXES) spectra of SrTiO<sub>3-δ</sub> ( $\delta = 0, 0.02$ ). For reference, the PES spectra were also measured. The SXES spectra reflect the electronic structure of the bulk compared with PES spectra, because the mean free path of a soft-X-ray is very long compared with that of the electron. Furthermore, the Raman

scattering observed in the SXES spectra provides useful information about the electronic structure. It is reported that the Raman scattering for 3*d* transition metal compounds is attributed primarily to the  $d$ - $d$  transition between the 3*d* valence and conduction bands as well as charge transfer (CT) transition from an occupied O 2*p* band to an unoccupied 3*d* band.<sup>15–19</sup> Here, we prove that the ~1.5 eV peak in the band gap region of SrTiO<sub>3-δ</sub> exists as a bulk state, even though a surface state may also exist.

The SrTiO<sub>3-δ</sub> ( $\delta = 0, 0.02$ ) samples were prepared by the solid state reaction of SrCO<sub>3</sub> and TiO<sub>2</sub> at 1200°C for about 12 h, and the single crystals were grown by a floating-zone method using an Xe-arc imaging furnace. The SrTiO<sub>2.98</sub> crystal was obtained in an as-grown sample. The SrTiO<sub>3</sub> crystal was obtained by annealing the as-grown crystal in O<sub>2</sub> atmosphere at 800°C. The prepared crystals were examined by X-ray diffraction.

SXES spectra were measured using a soft-X-ray spectrometer installed at an undulator beamline BL-19B (at the Photon Factory), of the High Energy Accelerator Organization. Synchrotron radiation was monochromatized using a varied line spacing plane grating whose average groove density is 1000 lines/mm. The incidence angle of the soft-X-ray was selected to be about 75° in order to avoid the self-absorption effect. The energy resolution was smaller than 0.8 eV at  $h\nu = 450$  eV. The bottom axis was calibrated by measuring a 4*f* core level of Au.

Figure 1 shows the Ti 2*p* XAS spectrum of SrTiO<sub>2.98</sub>. The spectrum is mainly derived from two parts of  $L_3$  (2*p*<sub>3/2</sub>) and  $L_2$  (2*p*<sub>1/2</sub>). Each part is split into  $t_{2g}$  and  $e_g$  states by an octahedral ligand field. The spectrum is similar to those of SrTiO<sub>3</sub> and Sr<sub>1-x</sub>La<sub>x</sub>TiO<sub>3</sub>.<sup>17,19</sup> The vertical bars labeled from 1 to 6 indicate photon energies selected for resonant SXES measurements.

Figure 2 shows Ti 2*p* SXES spectra of SrTiO<sub>2.98</sub> excited at each point of Fig. 1. It is well known that the Ti 2*p* emission reflects the Ti 3*d* partial density of states. An arrow shown in each spectrum is attributed to elastic scattering of the excitation photon. The elastic peak is enhanced at the excitation energy corresponding to the  $t_{2g}$  absorption peak of  $L_3$ . Then, the peak intensity decreases with increasing excitation energy.

The SXES spectrum 6 excited at  $h\nu = 472$  eV is an off-

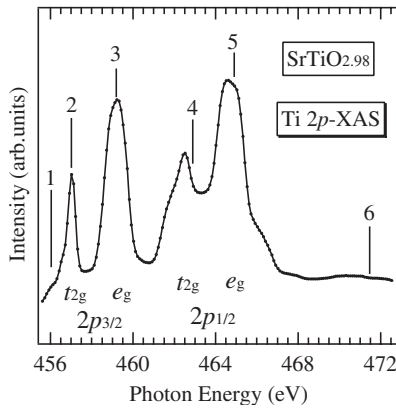


Fig. 1. Ti 2p XAS spectra of SrTiO<sub>2.98</sub>. The numbers indicate the photon energies where the Ti 2p SXES spectra were measured.

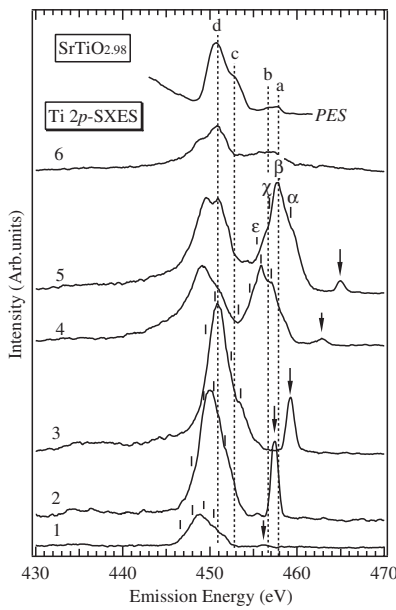


Fig. 2. Ti 2p SXES spectra of SrTiO<sub>2.98</sub> excited at various photon energies in Fig. 1. Arrow shows the energy position of the excitations photon energy. Vertical broken lines show the energy positions of Ti 3d → 2p fluorescence. For reference, the PES spectrum of SrTiO<sub>2.98</sub> is also shown.

resonance spectrum attributed to the normal Ti 3d → 2p fluorescence spectrum. This spectrum suggests that the Ti 3d state hybridizes with the O 2p state in the valence band. Four dashed lines (a, b, c, and d peaks) show the fluorescence bands. In the figure, the PES spectrum of SrTiO<sub>2.98</sub> is also shown above the fluorescence spectrum. It is striking that the energy positions of the fluorescence spectrum are in good agreement with those of the PES spectrum. Therefore, the a and b peaks correspond to the bonding state and the nonbonding state in the valence band, respectively. The c and d peaks correspond to the coherent band and the incoherent band in the band gap, respectively. On the other hand, a prominent feature at 448 eV may be due to the contribution of a satellite-like structure, though the origin is not clear.

Four parts ( $\alpha$ ,  $\beta$ ,  $\chi$ , and  $\varepsilon$ ) denoted by small vertical bars in each Ti 2p SXES spectrum represent the energy sites shifted from the excitation energy shown in Fig. 1, to be 5.6,

6.9, 8.0, and 9.3 eV, respectively. They shift as the excitation energy is varied. These features are attributed to the soft-X-ray Raman scattering (or inelastic scattering). The soft-X-ray Raman scattering that is excited in the  $L_3$  absorption spectral region overlaps with the Ti 3d → 2p fluorescence. The SXES spectrum 1 excited immediately below the Ti 2p threshold shows an apparent feature at a lower energy than the elastic scattering. Since the excitation energy is lower than the binding energy of Ti 2p, the Ti 3d → 2p fluorescence cannot be observed. It is attributed to a normal Raman scattering, where the intermediate is a virtual state. Similar features have already been observed in the SXES spectra of La<sub>0.10</sub>Sr<sub>0.90</sub>TiO<sub>3</sub>.<sup>17-19)</sup>

Figure 3(a) shows SXES spectra of SrTiO<sub>2.98</sub>, where the abscissa is the Raman shift (or energy loss) that is the energy shift from the elastic scattering. The energy of each elastic scattering peak in Fig. 2 is normalized at 0 eV in Fig. 3(a). The Ti 3d → 2p fluorescence peaks shown by four vertical bars (a, b, c, and d peaks) shift to the higher energy with increasing the excitation energy. Four dashed lines  $\alpha$ ,  $\beta$ ,  $\chi$ , and  $\varepsilon$  indicate the Raman scatterings. These Raman scatterings can be compared with the optical conductivity spectrum,<sup>3)</sup> since the elementary excitation of the Raman scattering is the valence band transition. Therefore, the optical conductivity spectrum of SrTiO<sub>2.98</sub> is shown in Fig. 3(b). Compared with the SXES spectra, the four Raman scatterings are in good accordance with the optical conductivity spectrum, as shown by the four dashed lines. This fact indicates that these Raman scatterings can be attributed to a charge-transfer (CT) transition from the occupied O 2p state to the unoccupied Ti 3d state.<sup>17-19)</sup>

Figure 4 shows a comparison of the  $t_{2g}$ -resonanced SXES spectra between SrTiO<sub>3</sub> and SrTiO<sub>2.98</sub>. The  $\delta t_{2g}$  peak is

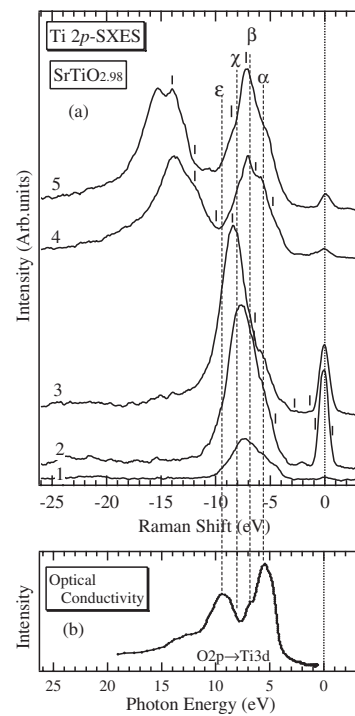


Fig. 3. (a) Ti 3d → 2p SXES spectra of SrTiO<sub>2.98</sub> presented as the relative emission energy to the elastic scattering. (b) Optical conductivity spectrum of SrTiO<sub>2.98</sub>.

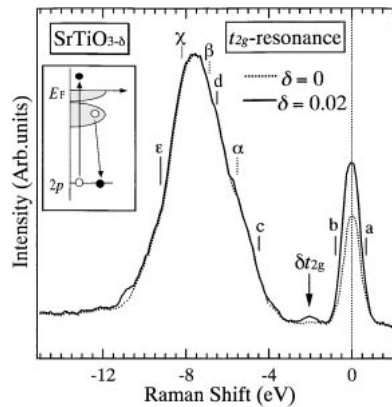


Fig. 4. Comparison of the  $t_{2g}$ -resonance SXES spectra of  $\text{SrTiO}_{2.98}$  and pure  $\text{SrTiO}_3$ . This  $t_{2g}$ -resonance spectrum obtained for  $\text{SrTiO}_{3-\delta}$  is spectrum 2 in Fig. 3.

observed at about 2.0 eV in  $\text{SrTiO}_{2.98}$ , though the peak is not observed in  $\text{SrTiO}_3$ . The PES in Fig. 2 indicates that two peaks attributed to Ti 3d states are observed just below the Fermi level ( $E_F$ ). The peaks are the coherent band at  $E_F$  and the incoherent band at about 1.5 eV below  $E_F$ . Their schematic energy states are inserted into Fig. 4. In the  $t_{2g}$  excitation, there is typically no large band splitting so that the contribution to the Raman scattering is due to the electron correlation energy ( $U_{dd}$ ). The Raman scattering of the  $\delta t_{2g}$  peak at approximately  $\sim 2.0$  eV corresponds to the  $d-d$  transition from the occupied incoherent band to the unoccupied coherent band. Therefore, the Raman shift of the  $\delta t_{2g}$  peak reflects the effective  $U_{dd}/2$ . The magnitude is in good agreement with the results of the PES and inverse-PES studies.<sup>11)</sup> On the other hand, the intensity at Raman shift = 0 eV is larger in  $\text{SrTiO}_{2.98}$ . This behavior indicates the Drude photoresponse which is attributed to the  $d-d$  transition between the coherent bands.<sup>19)</sup>

Recently, Kajueter *et al.* indicated that the degree of correlation and disorder is larger at the surface than that in the bulk.<sup>12)</sup> This finding explains an origin of the incoherent peak at  $\sim 1.5$  eV below the  $E_F$  in the PES spectra. However, the present results suggest that the  $\delta t_{2g}$  peak arises from the bulk state, even though the surface state may also contribute to it.

In conclusion, we have studied the electronic structure in the bulk state of  $\text{SrTiO}_{3-\delta}$  using the SXES technique. The electronic structure in the valence band region of the SXES spectrum reflects that of the PES spectrum. The CT Raman

scattering, which corresponds to the transition from O 2p to Ti 3d states in the virtual state, agrees with the optical conductivity spectrum. The Raman scattering, which is attributed to the  $d-d$  transition between the incoherent and the coherent bands, is directly observed in the  $t_{2g}$ -resonance SXES spectra of  $\text{SrTiO}_{3-\delta}$ . The Raman shift corresponds to the magnitude of the effective  $U_{dd}/2$ .

This work was partly supported by the Sumitomo Foundation and the Foundation for Materials Science and Technology of Japan (MST Foundation).

- 1) M. Imada, A. Fujimori and Y. Tokura: Rev. Mod. Phys. **70** (1999) 1039.
- 2) Y. Tokura, Y. Taguchi, Y. Okada, T. Arima, K. Kumagai and Y. Iye: Phys. Rev. Lett. **70** (1993) 2126.
- 3) Y. Fujishima, Y. Tokura, T. Arima and S. Uchida: Phys. Rev. B **46** (1992) 11167.
- 4) Y. Taguchi, T. Okuda, M. Ohashi, C. Murayama, N. Mohri, Y. Iye and Y. Tokura: Phys. Rev. B **59** (1999) 7917.
- 5) A. Fujimori, I. Hase, M. Nakamura, H. Namatame, Y. Fujishima and Y. Tokura: Phys. Rev. B **46** (1992) 9841.
- 6) A. Fujimori, A. E. Bocquet, K. Morikawa, K. Kobayashi, T. Saitoh, Y. Tokura, I. Hase and M. Onoda: J. Phys. Chem. Solids **57** (1996) 1379.
- 7) T. Higuchi, T. Tsukamoto, N. Sata, M. Ishigame, Y. Tezuka and S. Shin: Phys. Rev. B **57** (1998) 6978.
- 8) T. Higuchi, T. Tsukamoto, K. Kobayashi, Y. Ishiwata, M. Fujisawa, T. Yokoya, S. Yamaguchi and S. Shin: Phys. Rev. B **61** (2000) 12860.
- 9) A. Fujimori, T. Yoshida, K. Okazaki, T. Tsujioka, K. Kobayashi, T. Mizokawa, M. Onoda, T. Katsufuji, Y. Taguchi and Y. Tokura: J. Electron Spectrosc. Relat. Phenom. **117-118** (2001) 277.
- 10) Y. Aiura, I. Hase, H. Bando, T. Yasue, T. Saitoh and D. S. Dessau: Surf. Sci. **515** (2002) 61.
- 11) D. D. Sarma, S. R. Barman, H. Kajueter and G. Kotliar: Europhys. Lett. **36** (1996) 307.
- 12) H. Kajueter, G. Kotliar, D. D. Sarma and S. R. Barman: Int. J. Mod. Phys. B **11** (1997) 3849.
- 13) K. Maiti, P. Mahadevan and D. D. Sarma: Phys. Rev. Lett. **80** (1998) 2885.
- 14) N. Shanthi and D. D. Sarma: Phys. Rev. B **57** (1998) 2153.
- 15) S. M. Butorin, J.-H. Guo, M. Magnuson and J. Nordgren: Phys. Rev. B **55** (1997) 4242.
- 16) S. Shin, M. Fujisawa, H. Ishii, Y. Harada, M. Watanabe, M. M. Grush, T. A. Callcott, R. C. Perera, E. Z. Kurmaev, A. Moewes, R. Winarski, S. Stadler and D. L. Ederer: J. Electron Spectrosc. Relat. Phenom. **92** (1998) 197.
- 17) T. Higuchi, T. Tsukamoto, M. Watanabe, M. M. Grush, T. A. Callcott, R. C. Perera, D. L. Ederer, Y. Tokura, Y. Harada, Y. Tezuka and S. Shin: Phys. Rev. B **60** (1999) 7711.
- 18) A. Kotani and S. Shin: Rev. Mod. Phys. **73** (2001) 203.
- 19) T. Higuchi, T. Takeuchi, T. Tsukamoto, Y. Harada, Y. Taguchi, Y. Tokura and S. Shin: Nucl. Instrum. & Methods B **199** (2003) 386.